

Infraorbital groove localisation for the endoscopic decompression of the orbit in Graves' disease

A. Przygocka¹, K. Jędrzejewski², J. Szymański², G. Wyśiadecki³, M. Topol², M. Polgaj¹

¹Department of Angiology, Chair of Anatomy, Medical University of Lodz, Poland

²Department of Normal and Clinical Anatomy, Chair of Anatomy, Medical University of Lodz, Poland

³Department of Normal Anatomy, Chair of Anatomy, Medical University of Lodz, Poland

[Received 17 June 2014; Accepted 27 June 2014]

Background: The aim of our study was to determine the localisation of the inferior margin of the optic canal in relation to the infraorbital canal/groove complex (IOC/G complex) and zygomaticoorbitale (ZO) as the potential useful landmarks for reducing dangerous complications following surgical and invasive procedures.

Materials and methods: Sixty-four orbits of thirty-two human skulls were investigated. The distances between: the inferior margin of the optic canal and the posterior margin of the infraorbital groove measured at its medial border (OC-S); the inferior margin of the optic canal and the posterior margin of the roof of the infraorbital canal (OC-C); the inferior margin of the optic canal and the zygomaticoorbitale (OC-ZO) — were measured. The left/right symmetry ratio and the asymmetry index were counted. The symmetry between the contralateral measurements was analysed and statistical analysis was performed.

Results: On the right side the mean distance from the inferior margin of the optic canal to: the posterior margin of the infraorbital groove measured at its medial border; to the posterior margin of the roof of the infraorbital canal; and to the zygomaticoorbitale were: 23.41 ± 3.10 mm; 34.44 ± 5.30 mm; and 47.53 ± 4.13 mm, respectively. On the left side the mean distance from the inferior margin of the optic canal to: the posterior margin of the infraorbital groove measured at its medial border; to the posterior margin of the roof of the infraorbital canal; to the zygomaticoorbitale were 23.69 ± 2.80 mm; 36.75 ± 5.10 mm; 46.84 ± 3.24 mm, respectively.

Conclusions: The presented measurements may be particularly helpful for endoscopic decompression in patients with the thyroid ophthalmopathy to avoid the complications. (*Folia Morphol* 2015; 74, 1: 78–83)

Key words: morphometry, infraorbital groove, optic canal, orbital floor, orbital apex syndrome, thyroid ophthalmopathy, endoscopic orbital decompression

INTRODUCTION

Although the treatment of “thyroid eye disease” is based on obtaining a euthyroid state and include oral corticosteroids, retrobulbar corticosteroids,

orbital radiotherapy — the surgical decompression of the orbit is indicated for patients who are resistant to medical treatment, for compressive optic neuropathy or when contraindications to

corticosteroids or radiation treatments exist [5, 16, 31, 39, 48].

Surgical decompression of the orbit should be performed in non-traumatic manner by avoiding external incisions and allowing optimal visualisation of all important landmarks. The endoscopic approach allows surgeons to perform complete medial orbital wall decompression with excellent visualisation of the key landmarks. Only the portion of the orbital floor that lies medially to the infraorbital nerve should be removed [2–4, 25, 27, 39, 46–49].

The orbital apex is a place of communication between the orbit and the middle cranial fossa via the optic canal and the superior orbital fissure. There is a high concentration of important structures in the narrow space of the orbital apex in the neighbourhood of the optic canal, superior orbital fissure and the infraorbital canal/groove (IOC/G) complex [42, 50]. The IOC/G complex is the pathway for the infraorbital bundle and it is an important landmark in the endoscopic transnasal decompression for the thyroid ophthalmopathy and other maxillofacial techniques: the Caldwell-Luc procedure [39], the Walsh-Ogura procedure [48], tumour surgery of the maxilla, rhinoplasty, malar fractures, the Le Fort I type osteotomies and others [1, 6, 14, 19, 23, 26, 28, 34–37].

The aim of our study was to determine the localisation of the IOC/G complex in relation to the inferior margin of the optic canal for reducing dangerous complications following surgical and invasive procedures.

MATERIALS AND METHODS

Measurements were made on 64 orbits of 32 human dry skulls from the Chair of Anatomy of the Medical University of Lodz, Poland. The samples were from Polish population. The variables of age and gender were not considered.

The following morphometric measurements were collected (Fig. 1):

1. OC-S — the distance between the inferior margin of the optic canal and the posterior margin of the infraorbital groove measured at its medial border;
2. OC-C — the distance between the inferior margin of the optic canal and the posterior margin of the roof of the infraorbital canal;
3. OC-ZO — the distance between the inferior margin of the optic canal and the zygomaticoorbitale.

All measurements were tabulated and separated by side.

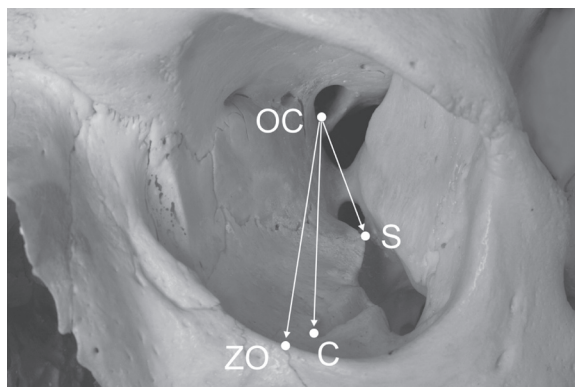


Figure 1. The human skull. Osteometric points in the orbit: OC — the inferior margin of the optic canal; C — the anterior margin of the infraorbital groove = the posterior margin of the roof of the infraorbital canal; S — the posterior margin of the infraorbital groove measured at its medial side. Osteometric measurements: OC-S — the distance between the inferior margin of the optic canal and the posterior margin of the infraorbital groove measured at its medial border; OC-C — the distance between the inferior margin of the optic canal and the posterior margin of the roof of the infraorbital canal; OC-ZO — the distance between the inferior margin optic canal and the zygomaticoorbitale.

The two more parameters were also calculated:

1. SR — the left/right symmetry ratio — calculated using the formula [30]:

$$SR = \frac{\text{Left parameter}}{\text{Right parameter}}$$

The SR = 0 indicates the perfect symmetry; the SR < 1 means that the right parameter is greater than the left one; the SR > 1 suggests that the left measurement is greater than the measurement on the opposite side.

2. AI — the asymmetry index — was counted for all parameters using the following formula [41]:

$$AI = \frac{\text{Right parameter} - \text{Left parameter}}{\text{Right parameter}} \times 100$$

As the right side parameters was used as reference — in such a case the negative values mean that corresponding distances on the left side were greater than on the right side. The minus symbol was not considered for the statistics.

RESULTS

The 64 orbits were studied (32 human skulls). On the right side the mean distance between the inferior margin of the optic canal and: the posterior margin of

Table 1. Anthropometric measurements of the human skulls collected in the current study

Distances [mm]		No.	Minimum	Maximum	Mean \pm SD	Median
OC-S	Right	32	17	30	23.41 \pm 3.10	23.5
	Left	32	19	30	23.69 \pm 2.80	24.0
OC-C	Right	32	23	46	34.44 \pm 5.30	34.5
	Left	32	30	47	36.75 \pm 5.10	36.0
OC-ZO	Right	32	41	55	47.53 \pm 4.13	48.0
	Left	32	41	52	46.84 \pm 3.24	48.0

SD — standard deviation; other abbreviations as in Figure 1.

Table 2. Symmetry/asymmetry of anthropometric measurements

Distance		0 mm	1 mm	2 mm	3 mm	4 mm	\geq 5 mm
OC-S	Right	4 (12.6%)	3 (9.4%)	3 (9.4%)	1 (3.1%)	–	3 (9.4%)
	Left		6 (18.7%)	6 (18.7%)	5 (15.6%)	1 (3.1%)	–
OC-C	Right	2 (6.2%)	3 (9.4%)	2 (6.2%)	3 (9.4%)	1 (3.1%)	–
	Left		4 (12.6%)	3 (9.4%)	3 (9.4%)	2 (6.2%)	9 (28.1%)
OC-ZO	Right	8 (25.0%)	4 (12.6%)	6 (18.8%)	2 (6.2%)	1 (3.1%)	1 (3.1%)
	Left		5 (15.7%)	2 (6.2%)	1 (3.1%)	1 (3.1%)	1 (3.1%)

Abbreviations as in Figure 1.

the infraorbital groove measured at its medial border; the posterior margin of the roof of the infraorbital canal; the zygomaticoorbitale were 23.41 \pm 3.10 mm; 34.44 \pm 5.30 mm; 47.53 \pm 4.13 mm, respectively. Comparing data on the left side we found that the left mean distances were: 23.69 \pm 2.80 mm; 36.75 \pm 5.10 mm; 46.84 \pm 3.24 mm, respectively (Table 1). The minimal and maximal OC-S distances were shorter than the OC-C distances. The minimal OC-ZO distances were the same on the left and on the right side. No OC-S asymmetry was observed in 12.6% of the samples, no OC-C asymmetry in 6.2% of the samples. An asymmetry of 1–2 mm was found in 18.8% for the right OC-S and in 37.4% for the left OC-S and it appeared more often than higher asymmetry of the OC-S distance on the right or on the left side. We noticed that the left OC-C distances were more often greater than the OC-C distances on the right side, furthermore the asymmetry of 5 mm and more on the left side was found in 28.1% in our study. No OC-ZO asymmetry was found in 25.0% of the samples and an asymmetry of 1–2 mm was found in 31.4% for the right OC-ZO and in 21.9% for the left OC-ZO measurements. The complete symmetry/asymmetry data are summarised in Table 2.

Table 3. The left/right symmetry ratio (SR)

Left/right SR	OC-S	OC-C	OC-ZO
SR = 1	4 (12.50%)	2 (6.25%)	8 (25.00%)
SR > 1	18 (56.25%)	21 (65.63%)	9 (28.13%)
SR < 1	10 (31.25%)	9 (28.13%)	15 (46.88%)

Abbreviations as in Figure 1.

Table 4. Asymmetry indexes (AI)

AI	OC-S	OC-C	OC-ZO
AI = 0	4 (12.50%)	2 (6.25%)	8 (25.00%)
AI > 0	10 (31.25%)	9 (28.13%)	15 (46.88%)
AI < 0	18 (56.25%)	21 (65.63%)	9 (28.13%)

Abbreviations as in Figure 1.

Left/right SR showed the total symmetry of OC-S, OC-C and OC-ZO parameters on both sides in 12.5%, 6.25% and 25.0%, respectively (Table 3). The AI showed that the left side distances were greater in 56.25%, 65.63%, and 28.13% for the OC-S, OC-C and OC-ZO parameters, respectively (Table 4).

DISCUSSION

Graves' ophthalmopathy — also known as Graves' orbitopathy (GO) or thyroid associated ophthalmopathy — is the most common cause of unilateral or bilateral proptosis in adults and may result in severe complications such as: widening of the palpebral fissure and exposure keratopathy, corneal ulceration, optic nerve compression and blindness, extraocular motility abnormalities, diplopia, strabismus and others [3, 4, 10, 27, 29, 31, 39, 43–45]. Thyroid ophthalmopathy is the most frequent cause of orbital disease in the adult population, responsible for 15% to 28% of cases of unilateral and 80% of cases of bilateral exophthalmia [8, 15, 29]. Optic neuropathy is an uncommon manifestation which occurs with rate of incidence ranging from 2% to 8.6% of patients with Graves' ophthalmopathy but causes severe complications [7, 38, 47].

Surgical decompression is a main treatment for GO resistant to the medical treatment. The primary goal of orbital decompression is to remove parts of the walls of the orbit to accommodate the increased volume of orbital tissue. This results in reduction of proptosis, decreased optic nerve compression or stretch and resolution of most of the symptoms [3, 4, 22, 47].

Historically, various approaches have been described in the literature (Table 5). Different types of surgical procedures include: removal of lateral, superior, medial wall of the orbit, complete or partial removal of the floor of the orbit or partial removal of the orbital floor with removal of the medial wall [3, 4, 40]. Dollinger [13] performed the orbital decompression by removing the lateral orbitotomy for exophthalmos as early as in 1911. Other approaches were described by Naffziger, Sewall and Hirsch. A new technique for decompressing the orbital contents transantrally into the maxillary sinus and the ethmoid space was proposed by Walsh and Ogura in 1957 [48]. In 1990 Kennedy et al. [25], first proposed to perform the Ogura technique transnasally under endoscopic guidance [13, 24, 25, 48] (Table 5).

The endoscopic approach allows performing complete medial orbital wall decompression with excellent visualisation of the key anatomic landmarks. Endoscopes permit a maximal posterior orbital decompression at the orbital apex which is difficult to access via transantral routes [3, 4, 25, 48]. Ocular recession from endoscopic decompression alone ranges from 2 mm to 12 mm. Additional concurrent lateral decompression to endoscopic procedure provides extra 2 mm of globe recession [2, 33].

Table 5. History of various approaches for the orbital decompression in Graves' ophthalmopathy

Year	Publication	Description
1911	Dollinger	First lateral orbitotomy for exophthalmos, modelled after Kronlein's procedure
1931	Naffziger	The orbital roof approach
1936	Sewell	The medial wall removal through an external ethmoidectomy approach
1950	Hirsch	An inferior orbitotomy approach
1957	Walsh and Ogura	Transantral Caldwell-Luc approach to decompress the medial and inferior orbital walls
1990	Kennedy	Proposed the Ogura technique transnasally under the endoscopic guidance

The safe limits for the orbital dissection are described in the literature and the term 'safe distances' is used [9, 11, 17]. However, the observation made in our study is difficult to compare with other studies because differences described in the literature are based on the type of population, chosen landmarks and also methods of measurements. The distance from the orbital rim to the important soft tissue of the orbital apex was investigated by Danko and Haug [12]. The mean distance was 44.1 ± 1.4 mm medially, 38.3 ± 3.0 mm laterally, 44.5 ± 1.72 mm superiorly, and 39.4 ± 2.9 mm inferiorly. No distance was less than 31.0 mm or exceeded 51.1 mm in their study. The 41 skulls of adult Koreans were measured by Hwang and Baik [17]. They described safe distances as following: 26.4 ± 2.6 mm from the infraorbital fissure where the infraorbital groove started to the infraorbital foramen; 34.3 ± 2.7 mm from the supraorbital fissure to the frontozygomatic suture; 31.7 ± 3.0 mm from the anterior lacrimal crest to the posterior ethmoidal foramen; and 40.0 ± 2.5 mm from the supraorbital fissure to the supraorbital notch [17]. Rontal et al. [40] studied 24 Indian skulls. They recommended that the safe distances for dissection were: inferiorly — 25 mm from the infraorbital foramen; laterally — 25 mm from the frontozygomatic suture; superiorly — 30 mm from the supraorbital notch; medially — 30 mm from the anterior lacrimal crest [40].

Ji et al. [18] described the orbital floor length defined as the distance between the optic foramen and the inferior junction between the inferior orbital rim and the perpendicular bisector line of the orbital bre-

adth: 47.00 ± 2.75 mm on the left side and 46.85 ± 2.81 mm on the right side. They found the average distances as 47.93 mm in men and 46.18 mm in women [18]. Karakas et al. [21] measured 62 orbits of 31 male Caucasian adults. They described the distances from the infraorbital foramen to the midpoint of the lateral margin of the lacrimal fossa — 23.8 ± 7.2 mm; to the inferior orbital fissure — 31.9 ± 3.9 mm and to the inferior orbital rim — 6.7 ± 1.9 mm and to the inferior aspect of the optic canal — 50.3 ± 3.2 mm [15, 19]. Those data are difficult to compare with data of our study as authors choose different landmarks. Huanmanop et al. [16] showed the average distance between the inferior border of the optic canal and the orbital rim above the infraorbital foramen measured 46.5 ± 2.8 mm on the right and 45.9 ± 2.8 mm on the left. The studies also showed that average distance between the orbital rim above the infraorbital foramen and the posterior margin of the roof of the infraorbital canal measured 12.3 ± 4.1 mm on the right and 12.4 ± 3.4 mm on the left [16]. McQueen et al. [32] measured 54 orbits. They measured distances from the orbital rim above the infraorbital foramen to the three landmarks: the optic canal — 49.73 ± 2.71 mm, the inferior orbital fissure — 37.43 ± 4.13 mm and to the posterior margin of the covering of the infraorbital canal — 17.08 ± 3.64 mm [32].

We can try to compare some data from the studies described above but it is still a matter of the chosen landmarks, so our measurement could not be directly compared with those mentioned in the literature as we chose different landmarks for our study to obtain new data important in orbital surgery. All the measurements mentioned above are useful in orbital surgery. In our opinion the landmarks relating to the infraorbital groove and the apex of the orbit may be of the utmost importance in the endoscopic decompression of the orbit, as they can be visualised during endoscopic manipulations.

Nowadays, orbital images obtained with three-dimensional computed tomography may be used as a method for gender evaluation [20] or anthropometric measurements of openings [8]. According to Kaplanoglu et al. [20], male had significantly wider and higher orbits. The right orbit was found to be wider than left. Burdan et al. [8] stated that the area of the right superior orbital fissure was insignificantly higher in males than in females. They observed reverse correlation on the left side.

CONCLUSIONS

Orbital surgeons should be aware of the morphometric relationships of the orbital floor due to the degree of variations. The boarder marked by IOC/G complex should not be passed and the safe distance to the apex of the orbit defined as the optic canal entrance should be kept. The distances between the entrance to the optic canal and the posterior end of the infraorbital groove — longer than given in our study are suspect to be safe but the distances to the zygomaticoorbitale should be minimal. New surgical methods and modified orbital approaches may be supported by checking new safe distances for surgical manipulations.

ACKNOWLEDGEMENTS

The paper was supported by grant No. 503/ /2-031-01/503-01 from the Medical University of Lodz, Poland.

REFERENCES

1. Aitasalo K, Kinnunen I, Palmgren J, Varpula M (2001) Repair of orbital floor fractures with bioactive glass implants. *J Oral Maxillofac Surg*, 59: 1390–1395.
2. Al-Mujaini A, Wali U, Alkhabori M (2009) Functional endoscopic sinus surgery: indications and complications in the ophthalmic field. *OMJ*, 24: 70–80.
3. Baradaranfar MH, Besharati (2002) Endoscopic decompression of orbit and optic nerve in Graves' disease: case report. *Acta Medica Iranica*, 40: 261–265.
4. Baradaranfar MH, Dabirmoghaddam P (2004) Transnasal endoscopic orbital decompression in Graves' ophthalmopathy. *Arch Iranian Med*, 7: 149–153.
5. Bartalena L, Baldeschi L, Dickinson A, Eckstein A, Kendall-Taylor P, Marcocci C, Mourits M, Perros P, Boboridis K, Boschi A, Currò N, Daumerie C, Kahaly GJ, Krassas GE, Lane CM, Lazarus JH, Marinò M, Nardi M, Neoh C, Orgiazzi J, Pearce S, Pinchera A, Pitz S, Salvi M, Sivelli P, Stahl M, von Arx G, Wiersinga WM; European Group on Graves' Orbitopathy (EUGOGO) (2008) Consensus Statement of the European Group on Graves' Orbitopathy (EUGOGO) on Management of the Graves' Orbitopathy. *Eur J Endocrinol*, 158: 273–285.
6. Brown M, Ky W, Lisman RD (1999) Concomitant Ocular Injuries With Orbital Fractures. *J Cranio-Maxillofacial Trauma*, 5: 41–46.
7. Burch H, Wartofsky L (1993) Graves' ophthalmopathy: current concepts regarding pathogenesis and management. *Endocrine Rev*, 14: 747–793.
8. Burdan F, Umlawska W, Dworzeński W, Klepacz R, Szumiło J, Starosławska E, Drop A (2011) Anatomical variances and dimensions of the superior orbital fissure and foramen ovale in adults. *Folia Morphol*, 70: 263–271.
9. Cakirer S, Cakirer D, Basak M, Durmaz S, Altuntas Y, Yigit U (2004) Evaluation of extraocular muscles in the edematous phase of Graves ophthalmopathy on contrast-enhanced fat-suppressed magnetic resonance imaging. *J Comput Assist Tomogr*, 28: 80–86.
10. Chen CT, Huang F, Chen YR (2006) Management of the Posttraumatic Enophthalmos. *Chang Gung Med J*, 29: 251–261.

11. Chien HF, Wu CH, Wen CY, Shieh JY (2001) Cadaveric study of blood supply to the lower intraorbital fat: etiologic relevance to the complication of anaerobic cellulitis in orbital floor fracture. *J Formos Med Assoc*, 100: 192–197.
12. Danko I, Haug RH (1998) An experimental investigation of the safe distance for internal orbital dissection. *J Oral Maxillofacial Surg*, 56: 749–752.
13. Dollinger J (1911) Die Druckenlastung der augenhohle durch entfernung der ausseren orbitalwand bei hochgradigem exophthalmus und konsekutiver hornhauterkrankung. *Dtsch Med Wochenschr*, 37: 1888–1890.
14. Ducic Y, Verret D (2009) Endoscopic transantral repair of orbital floor fractures. *Otolaryngology-Head Neck Surgery*, 140: 849–854.
15. El-Kaissi S, Frauman Ag, Wall JR (2004) Thyroid-associated ophthalmopathy: a practical guide to classification, natural history and management. *Intern Med J*, 34: 482–491.
16. Huanmanop T, Aghthong S, Chentanez V (2007) Surgical anatomy of fissures and foramina in the orbits of Thai adults. *J Med Assoc Thai*, 90: 2383–2391.
17. Hwang K, Baik SH (1999) Surgical anatomy of the orbit of Korean adults. *J Craniofac Surg*, 10: 129–134.
18. Ji Y, Qian Z, Dong Y, Zhou H, Fan X (2010) Quantitive morphometry of the orbit in Chinese adults based on a three-dimensional reconstruction method. *J Anat*, 217: 501–506.
19. Jin HR, Yeon JY, Shin SO, Choi YS (2007) Endoscopic versus external repair of orbital blowout fractures. *Otolaryngology-Head Neck Surgery*, 136: 38–44.
20. Kaplanoglu V, Kaplanoglu H, Toprak U, Parlak IS, Tatar IG, Deveer M, Hekimoglu B (2014) Anthropometric measurements of the orbita and gender prediction with three-dimensional computed tomography images. *Folia Morphol*, 73: 149–152.
21. Karakaş P, Bozkir MG, Oğuz Ö (2002) Morphometric measurements from various reference points in the orbit of male Caucasians. *Surg Radiol Anat*, 24: 358–362.
22. Kasperbauer JL, Hinkley L (2005) Endoscopic orbital decompression for Graves' ophthalmopathy. *Am J Rhinol*, 19: 603–606.
23. Kazkayasi M, Ergin A, Ersoy M, Tekdemir I, Elhan A (2003) Microscopic anatomy of the infraorbital canal, nerve, and foramen. *Otolaryngology-Head Neck Surgery*, 129: 692–697.
24. Kennedy DW (1985) Functional endoscopic sinus surgery. *Technique Arch Otolaryngol*, 111: 643–649.
25. Kennedy DW, Goodstein MD, Miller NR, Zinreich SJ (1990) Endoscopic transantral orbital decompression. *Arch Otolaryng Head Neck Surg*, 116: 275–282.
26. Kirsch E, Hammer B, von Arx G (2009) Graves' orbitopathy: current imaging procedures. *Swiss Med Wkly*, 139: 618–623.
27. Koay B, Bates G, Elston J (1997) Endoscopic orbital decompression for dysthyroid eye disease. *J Laryngol Otol*, 111: 946–949.
28. Lawrence JE, Poole MD (1992) Mid-facial sensation following craniofacial surgery. *Br J Plast Surg*, 45: 519–522.
29. Machado KFS, de Mattos Garcia M (2009) Thyroid ophthalmopathy revisited. *Radiol Bras*, 42: 261–266.
30. Maglione M, Constatinides F (2012) Localization of basicranium midline by submentoverte projection for the evaluation of condylar asymmetry. *Int J Dent*, 1–8.
31. Mallika PS, Tan AK, Aziz S, Syed Alwi SAR, Chong MS, Vanitha R, Intan G (2009) Thyroid associated ophthalmopathy: a review. *Malaysian Family Physician*, 4: 8–14.
32. McQueen C, DiRuggiero D, Cambell JP, Shockley W (1995) Orbital osteology: a study of the surgical landmarks. *Laryngoscope*, 105: 783–788.
33. Metson R, Dallow R, Shore J (1994) Endoscopic orbital decompression. *Laryngoscope*, 104: 950–957.
34. Meyer M, Moss A, Cullen K (1990) Infraorbital nerve palsy after rhinoplasty. *J Cranio Maxillofac Surg*, 18: 173–174.
35. Mozsary P, Middleton R (1983) Microsurgical reconstruction of the infraorbital nerves. *J Oral Maxillofac Surg*, 41: 697–700.
36. Przygocka A, Podgórski M, Jędrzejewski K, Topol M, Polguy M (2012) The location of the infraorbital foramen in human skulls to be used as new anthropometric landmarks as a useful method for maxillofacial surgery. *Folia Morphol*, 71: 198–204.
37. Przygocka A, Szymański J, Jakubczyk E, Jędrzejewski K, Topol M, Polguy M (2013) Variations in the topography of the infraorbital canal/groove complex: a proposal for classification and its potential usefulness in orbital floor surgery. *Folia Morphol*, 72: 311–317.
38. Riley FC (1972) Orbital pathology in Graves' disease. *Mayo Clin Proc*, 47: 975–979.
39. Rizk S, Papageorge A, Liberatore LA, Sacks EH (2000) Bilateral simultaneous orbital decompression for Graves orbitopathy with a combined endoscopic and Caldwell-Luc approach. *Otolaryngology-Head Neck Surgery*, 122: 216–221.
40. Rontal E, Rontal M, Guilford FT (1979) Surgical anatomy of the orbit. *Ann Otol Rhinol Laryngol*, 88: 382–386.
41. Rossi M, Ribeiro E, Smith R (2003) Craniofacial asymmetry in development: an anatomical study. *Angle Orthod*, 73: 381–385.
42. Scarfe WC, Langlais RP, Ohba T, Kawamata A, Maselle I (1998) Panoramic radiographic patterns of the infraorbital canal and anterior superior dental plexus. *Dentomaxillofac Radiol*, 27: 85–92.
43. Schotthoefer EO, Wallace DK (2007) Strabismus associated with thyroid eye disease. *Curr Opin Ophthalmol*, 18: 361–365.
44. Shah Y (2011) Thyroid ophthalmopathy. *Suppl JAPI*, 59: 60–65.
45. Singer P, Cooper D, Levy EG, Ladenson PW, Braverman LE, Daniels G, Greenspan FS, McDougall IR, Nikolai TF (1995) Treatment guidelines for patients with hyperthyroidism and hypothyroidism. *JAMA*, 273: 808–812.
46. Soares-Welch C, Fatourechhi V, Bartley GB, Beatty CW, Gorman CA, Bahn RS, Bergstralh EJ, Schleck CD, Garrity JA (2003) Optic neuropathy of Graves disease: results of transantral orbital decompression and long term follow up in 215 patients. *Am J Ophthalmol*, 136: 433–441.
47. Tang IP, Prepageran N, Subrayan V, Tajunisah I (2008) Endoscopic orbital decompression for optic neuropathy in thyroid ophthalmopathy. *Med J Malaysia*, 63: 337–338.
48. Walsh TE, Ogura JH (1957) Transantral orbital decompression for malignant exophthalmos. *Laryngoscope*, 67: 544–549.
49. Wee DT, Carney AS, Thorpe M, Wormald PJ (2002) Endoscopic orbital decompression for Graves' ophthalmopathy. *J Laryngol Otol*, 116: 6–9.
50. Yeh S, Foroozan R (2004) Orbital apex syndrome. *Curr Opin Ophthalmol*, 15: 490–498.